

## TiO<sub>2</sub>/KAOLIN COMPOSITE AS LOW-COST ADSORBENT FOR PROCION RED REMOVAL FROM AQUEOUS SOLUTION: KINETICS, EQUILIBRIUM, AND THERMODYNAMIC STUDIES

Tarmizi Taher<sup>1</sup>, Astriada Wulandari<sup>2</sup>, Risfidian Mohadi<sup>2</sup> and Aldes Lesbani<sup>1,2\*</sup>

<sup>1</sup>Department of Environmental Sciences, Graduate School of Universitas Sriwijaya, Jl. Padang Selasa, No. 524, Bukit Besar, Palembang 30139, South Sumatra, Indonesia

<sup>2</sup>Department of Chemistry, Faculty of Mathematics and Natural Sciences, Universitas Sriwijaya, Jl. Palembang-Prabumulih, Km. 32, Ogan Ilir, 30662, South Sumatra, Indonesia

(Received October 30, 2018; Revised August 10, 2019; Accepted August 15, 2019)

**ABSTRACT.** Procion red is one of the most utilized textile dyes by numerous textile factories worldwide. Unfortunately, it has a detrimental effect on the ecosystem whenever it was released into the environment as textile wastewater. In this work, the removal of procion red from aqueous solution has been conducted by adsorption with modified natural kaolin as a low-cost adsorbent. Kaolin was systematically modified by thermal activation then followed by acid activation in different acid concentration. Activated kaolin sample was then mixed with TiO<sub>2</sub> to produce TiO<sub>2</sub>/Kaolin composite. Activated kaolin and TiO<sub>2</sub>/Kaolin composite were characterized using X-ray diffraction (XRD) and Fourier transform infrared (FT-IR). Various operational variables that affect the adsorption process were taken into consideration, including the effect of initial pH, contact time, initial dye concentration, and temperature. The adsorption parameters of kinetics, isotherm, and thermodynamics were also studied according to the most common model established. The results showed that the procion red adsorption was pH-dependent and reached equilibrium at 90 min. The kinetics study was revealed that the adsorption process was better demonstrated by the pseudo-first-order rather than the pseudo-second-order model. The adsorption isotherm investigation showed that the adsorption process was followed both Langmuir and Freundlich model with  $q_s$  reached 158 mg/g, and the adsorption process was predicted in favorable condition. The thermodynamic study revealed that the adsorption process is spontaneous with endothermic nature. According to the results, it can be considered that the TiO<sub>2</sub>/Kaolin composite adsorbent has better adsorption capability to the procion red.

**KEY WORDS:** Activated kaolin, TiO<sub>2</sub>, Composite, Adsorption, Procion red

### INTRODUCTION

Nowadays, the reduction of freshwater quality affected by the discharge of numerous hazardous chemicals from various industrial and urbanization activities has become major worldwide issues [1]. The textile industry has a significant contribution to water pollution since it produces an extensive amount of colored wastewater [2]. The textile wastewater incorporates various synthetic dyes that have excessive color intensity, high chemical oxygen demand (COD), hardly degraded by natural condition, and high suspended solids [3]. Dyes used in the textile industry is commonly synthetic dyes, which are composed of complex organic molecules with a reactive functional group [4]. The release of dyes effluents into the aquatic environment is not only staining the water body but also causing COD increase, eutrophication and even human health problems owing to their high stability, toxicity, and mutagenic nature [5]. Consequently, the development of dyes effluent treatment methods is highly necessary to preserve environmental sustainability.

A number of methods have been developed in order to remove dyes contamination from wastewater, like adsorption [6], electrocoagulation [7], photovoltaic electrocoagulation [8], high-voltage pulsed discharge [9], flocculation [10], photocatalysis [11], ozonation [12], and

\*Corresponding author. [aldeslesbani@pps.unsri.ac.id](mailto:aldeslesbani@pps.unsri.ac.id)

This work is licensed under the Creative Commons Attribution 4.0 International License

advance oxidation [13]. However, the effort to completely remove dye pollutant is hard due to its high resistance and stability to the environmental condition [14]. Adsorption is considered as the most reliable and widely used method of dye removal from wastewater. It is an efficient, cheap, and eco-friendly technique compared with the other conventional techniques mentioned above due to the availability of various kind of adsorbent.

Kaolin is one of the most abundant and utilized natural clays. Basically, kaolin is mainly composed of kaolinite minerals with the chemical formula  $\text{Al}_2\text{Si}_2\text{O}_5(\text{OH})_4$  [15]. Its structure consists of two-layered of silicate ( $\text{SiO}_4$ ) tetrahedral and alumina ( $\text{AlO}_2(\text{OH})_4$ ) octahedral. Although theoretically, kaolin has no net surface charge, in the natural condition, it has a slight negative charge due to the defect on the edge of the crystalline structure [16]. Recently, many papers have been reported that the kaolin or kaolinite minerals had been widely used for various purposes such as fabrication of rubber, paper, plastic, cosmetics, coating, paints, and ceramics, the catalyst for the diverse chemical reaction, and adsorbent. These broad applications of kaolin are owing to its nifty nature, such as high cation exchange capacity, layered structure, and high thermal stability [17, 18].

In the present paper, we reported the natural kaolin modification by thermal and acid activation, followed by the preparation of  $\text{TiO}_2/\text{Kaolin}$  composite. The final  $\text{TiO}_2/\text{Kaolin}$  composite product then used as the adsorbent to remove Procion red dye as a model of dye pollutant.

## EXPERIMENTAL

### *Chemicals and instrumentation*

Kaolin used in this work was natural kaolin obtained from Waytuba kaolin deposit located in Waykanan District of Lampung Province, Indonesia. The raw kaolin sample was ground to gain adequate size for further treatment. The chemical composition of natural kaolin has been analyzed using X-ray fluorescence, and the result to be as follows: 34.7%  $\text{Al}_2\text{O}_3$ , 53.3%  $\text{SiO}_2$ , 4.25%  $\text{K}_2\text{O}$ , 0.05%  $\text{CaO}$ , 1.11%  $\text{TiO}_2$ , 4.47%  $\text{Fe}_2\text{O}_3$ , 0.57%  $\text{NiO}$ , 0.08%  $\text{CuO}$ , and 0.02%  $\text{ZnO}$ . Sulfuric acid (assay 99.999%) was supplied by Sigma-Aldrich (Singapore), and solid sodium hydroxide was purchased from Merck (Germany). Titanium(IV) isopropoxide as the titanium source was purchased from Sigma-Aldrich. All the chemical used was in reagent grade and used as received without further purification. The distilled water (conductivity of 18  $\text{M}\Omega/\text{cm}$ ) used for all the dilution was produced by Pureit<sup>®</sup> instrument. Procion red dye used as textile pollutant model was purchased from Sigma-Aldrich with dye content 40% and used as received without further purification. It has empirical chemical formula  $\text{C}_{19}\text{H}_{10}\text{Cl}_2\text{N}_6\text{Na}_2\text{O}_7\text{S}_2$  with the molecular weight of 615.33 g/mol, and its chemical structure was presented in Figure 1.

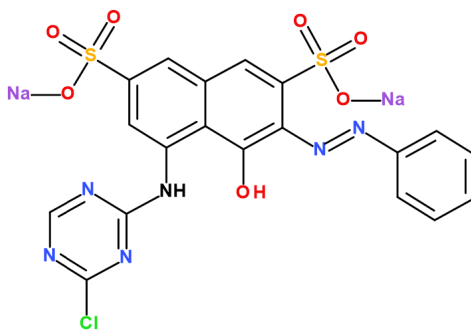


Figure 1. Chemical structure of Procion red.

The chemical composition of natural kaolin sample was analyzed using X-ray fluorescence provided by PANanalytical type Minipal 4. The chemical analyses of the natural and modified kaolin were carried out using XRD Rigaku Miniflex 600 with Ni-filtered CuK $\alpha$  irradiation. The change of the functional group of the kaolin sample was analyzed using FT-IR Shimadzu Prestige-21 using the KBr disc method in the wavenumber 400 to 4000 cm<sup>-1</sup>.

#### *Natural kaolin activation*

The activated kaolin was prepared by two-step activation process, i.e., thermal activation and followed by acid activation. Firstly, the natural kaolin (N-Kao) obtained was cleaned and crushed before subjected to the calcination process. Thermal activation method was carried out based on the work done by [19]. In brief, an amount of cleaned natural kaolin sample was subjected to a muffle furnace (Thermo Scientific) at temperature 500 °C for 3 h with a heating rate of 5 °C/min. After the calcination process finished, the samples then stored in a tightly closed bottle and labeled as TA-Kao.

Acid activation treatment was carried out to the thermally activated kaolin (TA-Kao). The acid activation process was conducted based on the work reported by Gao *et al.* [20] with slight modification. Firstly, TA-Kao sample was crushed and sieved to pass through 180 mesh particle size. Then, 3 g of the sieved TA-Kao was added into a three-neck flask containing 15 mL of H<sub>2</sub>SO<sub>4</sub> with different concentration (1, 5, 10, and 15%) in order to study the effect of the acid concentration on the kaolin structure. The mixture was then heated in mild condition (80 °C) under vigorous stirring for 12 h. After finished, the mixture was separated by centrifugation and washed using distilled water for several times to remove the excess of SO<sub>4</sub><sup>2-</sup>. Acid-activated kaolin product as filtrate then was dried at 50 °C followed by crushing and sieved to produce particle size < 80  $\mu$ m. The products were labeled as A-Kao 1%, A-Kao 5%, A-Kao 10%, and A-Kao 15% corresponding to the H<sub>2</sub>SO<sub>4</sub> concentration used during the activation process.

#### *Preparation TiO<sub>2</sub>/Kaolin composite*

TiO<sub>2</sub>/Kaolin composite was prepared using titanium(IV) isopropoxide as the source of titanium. The TiO<sub>2</sub> deposition on the surface of the kaolin was carried out by the following procedure. Approximately 3 g of activated kaolin sample A-Kao 10% was added to a beaker flask containing 100 mL of deionized water. The mixture was shaken for 2 h to obtain the kaolin suspension. In a separated flask, titanium solution was prepared by adding 80 mL of titanium(IV) isopropoxide with controlled-molar of the sulfuric acid solution. The titanium solution then drop-wisely added into the kaolin suspension. Then the mixture was stirred for 2 h at 50 °C. After finished, the mixture was separated by centrifugation followed by washing with deionized water for several times in order to remove the excess of SO<sub>4</sub><sup>2-</sup> ions and the other chemical impurities. The final product of TiO<sub>2</sub>/Kaolin composite then labelled as Ti/Kao and ready for further used as an adsorbent.

#### *Adsorption experiment*

Procion red solution as the model of textile wastewater with different concentration was prepared by diluting procion red stock solution (1000 mg/L). All the adsorption experiments were used the A-Kao 10% sample as the adsorbent and the adsorption process conducted based on the batch technique. In normal experiment, 50 mL of procion red solution (50 mg/L) was added into a canonical flask containing 0.05 g of adsorbent. The canonical flask was shaken for 190 min in a horizontal shaker with constant speed at 240 rpm. The effect of initial pH on the adsorption performance was studied in different initial pH condition ranging from 1 to 10. The investigation of the adsorption kinetics, equilibrium isotherm, and thermodynamic behavior was

performed at a different contact time, initial concentration, and adsorption temperature, respectively. After the batch experiment finished, the mixture was separated by centrifugation using Haniil® centrifuge instrument at 4000 rpm for 5 min. The remaining concentration of procion red in the supernatant was determined using EMCLAB UV-Vis spectrophotometer (Germany) at wavelength 538 nm. The whole experiments were conducted in duplicate in order to avoid the error of measurement and analysis. The amount of procion red adsorbed at time  $t$  was determined based on the following equation.

$$q_t = \frac{V}{m}(C_0 - C_t) \quad (1)$$

where  $q_t$  is the amount of procion red adsorbed per unit mass of adsorbent at the predetermined time (mg/g).  $C_0$  and  $C_t$  are the concentration of procion red at the initial and after adsorbed, respectively (mg/L).

For the equilibrium state, the adsorption capacity ( $q_e$ ) was determined based on the following equation.

$$q_e = \frac{V}{m}(C_0 - C_e) \quad (2)$$

where  $C_e$  is the concentration of procion red at the adsorption equilibrium condition (mg/L) and  $C_0$  is the initial concentration of procion red (mg/L).  $V$  is the volume of procion red solution used (L) and  $m$  is the amount of the adsorbent used (g).

## RESULTS AND DISCUSSION

### *Adsorbent characterization*

#### *XRD analysis*

The result of the XRD analysis of the natural kaolin sample is presented in Figure 2. The XRD pattern of natural kaolin described that natural kaolin sample was mainly composed by kaolinite mineral  $\text{Al}_2\text{Si}_2\text{O}_5(\text{OH})_4$  and the slight amount of quartz as impurities. The intense diffraction peaks were recorded at  $2\theta$  range of 5 to  $80^\circ$ . Moreover, the main characteristic reflection peaks of kaolinite were recorded at  $2\theta$  value of  $12^\circ$  and  $25^\circ$  as the reflections of the plane (001) [21]. After thermal activation at  $400^\circ\text{C}$ , the typical reflection peak of kaolin was not changed significantly (Figure 2). This finding showed that the thermal activation was not influenced the crystallinity of the kaolinite mineral.

The acid activation process was conducted with different acid concentration. The XRD patterns of acid-activated kaolin are presented in Figure 2a and the effect of acid concentration on the kaolinite characteristic reflection peak at  $2\theta$  around  $12^\circ$  and  $25^\circ$  is presented in Figure 2b. Figure 2b described that after acid activation the intensity of typical characteristic peaks of kaolinite at  $2\theta$  around  $12^\circ$  and  $25^\circ$  gradually changed. With relatively low acid concentration, the typical peak of kaolinite increased. However, with higher acid concentration it was gradually decreased as increasing the acid concentration. This phenomenon attributed to the partial mineral dilution due to the acid leaching that causing the disorder of kaolinite structure.

The XRD pattern of  $\text{TiO}_2/\text{Kaolin}$  composite is presented in Figure 2a. Compared with the XRD pattern of activated kaolin, it was significantly changed due to the deposition of  $\text{TiO}_2$  in the kaolin surface. The typical characteristic peak of kaolinite at  $12^\circ$  was disappeared as well as the other peaks of kaolinite. Moreover, the appearance of reflection peak at  $2\theta$  around 25, 37, 48, 55, and  $62^\circ$  indicated the presence of anatase [22]. Based on these results, we conclude that the  $\text{TiO}_2$  was systematically coated on the surface of kaolin.

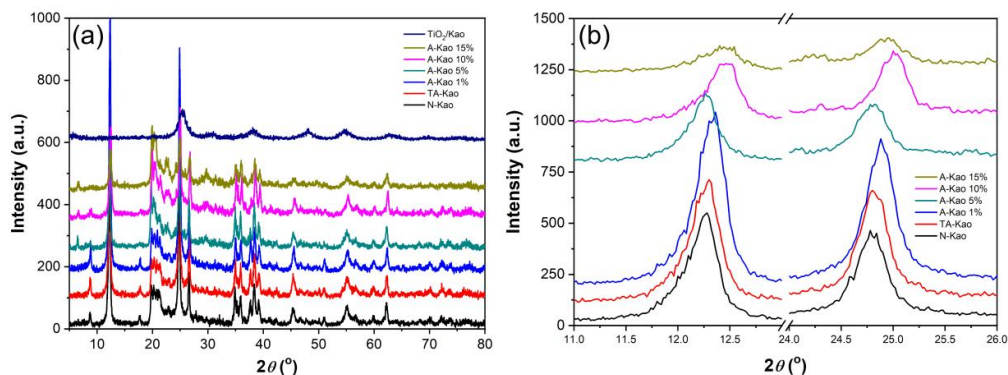


Figure 2. XRD pattern: (a) natural kaolin, activated kaolin, and TiO<sub>2</sub>/Kaolin composite and (b) the change of the main characteristic of the kaolin reflection peak at  $2\theta$  around  $12^\circ$  and  $25^\circ$  due to the activation process.

#### FT-IR analysis

The functional group of natural, activated kaolin, and TiO<sub>2</sub>/Kaolin composite were analyzed by FT-IR at the frequency range of 400–4000 cm<sup>-1</sup>. The FT-IR spectrum of natural kaolin was presented in Figure 3a. In the functional group region (4000–1100 cm<sup>-1</sup>) the band around 3448, 3618, and 3695 cm<sup>-1</sup> correspond to the O-H stretching vibration of Al-OH functional group. The sharp band at 3619 cm<sup>-1</sup> represent the hydroxyl group that presence between the tetrahedral and octahedral sheet. The presence of water that absorbed in the surface of the kaolin was described by the appearance of band observed at 3695 and 1635 cm<sup>-1</sup> [21]. The strong band recorded at 1111 cm<sup>-1</sup> corresponds to the Si-O stretching vibration. The sharp band at 918 cm<sup>-1</sup> corresponds to the characteristic stretching vibration of Al-Al-OH. While the characteristic band at 547 cm<sup>-1</sup> was correlated to the presence of Si-O-Al stretching vibration as the typical characteristic band of kaolinite mineral.

After thermal activation (Figure 3a), the band at the fingerprint region was not changed significantly. However, the band that related to the -OH group at 1635 cm<sup>-1</sup> and around 3600 cm<sup>-1</sup> was decreased. This finding showed that the water molecule that physisorbed in the kaolin surface was decreased.

The FT-IR spectra of acid-activated kaolin with different acid concentration are presented in Figure 3b. It showed that by increasing the acid concentration, the characteristic band at the region of the functional group was gradually decreased. This finding is in agreement with the results described by XRD analysis. By increasing the acid concentration, the partial destruction of the kaolinite structure has occurred.

The FT-IR spectra of TiO<sub>2</sub>/Kaolin composite is depicted in Figure 3a. Compared with the acid-activated kaolin spectra, the spectra of TiO<sub>2</sub>/Kaolin composite has changed significantly. Particularly, the band of activated kaolin at the fingerprint region disappeared. However, the characteristic band of 1111 cm<sup>-1</sup> still hang in there although its intensity was decreased significantly. This phenomenon indicated that during the compositing process, the TiO<sub>2</sub> was coating the kaolin surface. Hence, the structure of the kaolin was blocked by the presence of TiO<sub>2</sub> (anatase).

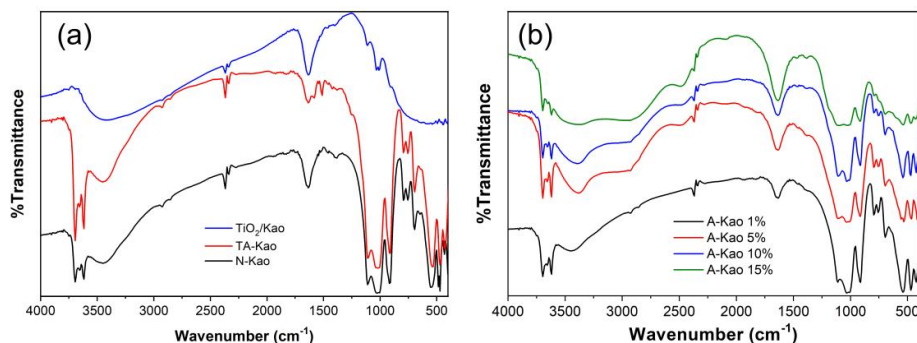


Figure 3. FTIR spectra of (a) natural kaolin, thermal activated kaolin, TiO<sub>2</sub>/Kaolin composite and (b) acid-activated kaolin at the different acid concentration.

#### *Effect of contact time*

The investigation on the effect of contact time toward the adsorption performance of procion red on natural and TiO<sub>2</sub>/Kaolin composite was systematically carried out. The adsorption experiment was set out with different contact time ranging from 0 to 90 min. The results of this investigation were illustrated in Figure 4. Based on the obtained result, the adsorption capacity of procion red both on activated kaolin and TiO<sub>2</sub>/Kaolin composite was gradually increased by increasing the contact time. However, after 50 min of contact time, the adsorption capacity slightly increased until it reached the equilibrium state at 90 min. At the equilibrium, the adsorption capacity of A-Kao reached 11.9 mg/g and for TiO<sub>2</sub>/Kaolin composite reached 13.1 mg/g. This finding indicates that the TiO<sub>2</sub>/Kaolin composite has better adsorption capability against procion red.

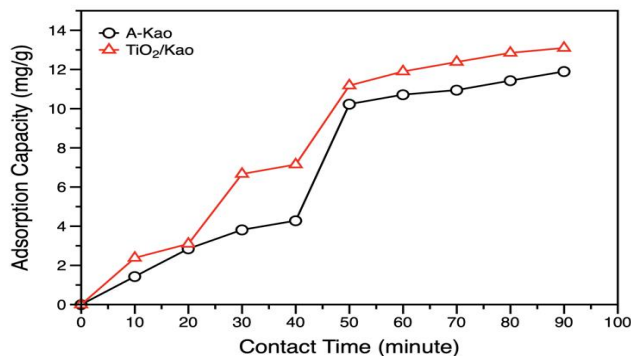


Figure 4. Effect of contact time on the adsorption performance.

#### *Effect of initial pH*

The influence of pH on the adsorption of procion red was systematically studied in various adsorption experiment with different initial pH condition. The pH of the dye solution was adjusted in the range of 1 to 9 by adding 0.1 M HCl and NaOH solution. The results of this study were illustrated in Figure 5a. The change of pH solution is an aspect that was significantly

affecting the adsorption performance. The change of pH in the solution will affect the nature of both dye solution and the surface of the adsorbent [14].

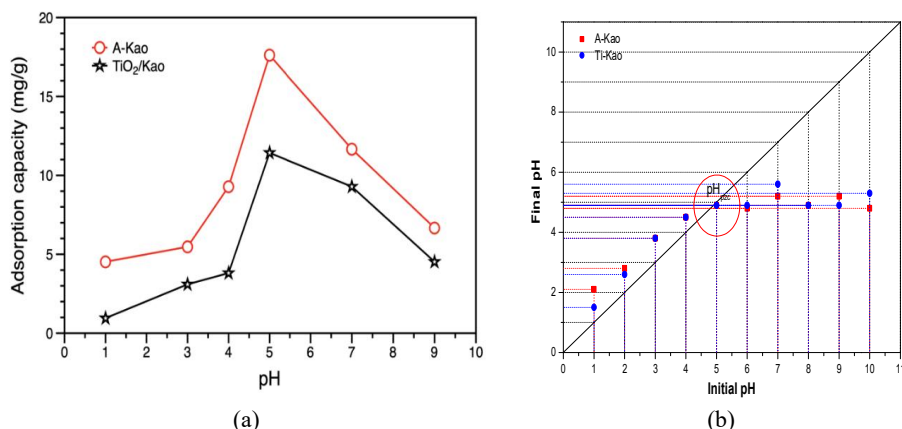


Figure 5. Effect of initial pH (a), and pH point zero charge ( $\text{pH}_{\text{pzc}}$ ) of activated kaolin and TiO<sub>2</sub>/Kaolin composite (b).

The maximum adsorption capacity of procion red on both adsorbents was observed at pH 5 (acidic pH). Theoretically, the surface of the kaolin has a slightly negative charge. Since the procion red is an anionic dye, in the acidic solution, the ionic strength of the procion red reduced then give rise to the higher probability to be adsorbed on the negatively charged surface. The chemistry of the adsorbent surface as the effect of change of pH solution can be described according to the point zero charge  $\text{pH}_{\text{pzc}}$  of the adsorbent. As can be seen in Figure 5b, the point zero charges of both adsorbents were recorded at pH 5. Below  $\text{pH}_{\text{pzc}}$  value, the surface of the adsorbent will be positively charged leading to the stronger electrostatic force toward the procion red which is an anionic dye. Above the  $\text{pH}_{\text{pzc}}$  value, the surface of the adsorbent will be negatively charged that causing the repulsion force toward the anionic procion red and causing the decrease of the adsorption performance.

#### Adsorption kinetics

The adsorption kinetics is an important aspect in order to investigate the design of the adsorption process and to evaluate the adsorbent behavior for procion red removal as a pollutant [23]. In order to correlate the adsorption kinetics data, the most common adsorption kinetics model was employed including the pseudo-first-order and pseudo-second-order models. The pseudo-first-order kinetic model was initiated and developed by [24], to study the adsorption mechanism for solid/liquid system. The nonlinear equation for the pseudo-first-order model can be described by the following equation:

$$q_t = q_e(1 - \exp^{-k_1 t}) \quad (3)$$

$$\frac{dq}{dt} = k_1(q_e - q_t) \quad (4)$$

The linear form of the pseudo-first-order model can be obtained by integrating equation 4 with applying boundaries condition of  $t = 0 - t$  and  $q = 0 - q_t$ . The results can be expressed as the following form[26]:

$$\log(q_e - q_t) = \log(q_e) - \frac{k_1}{2.303} t \quad (5)$$

where  $q_e$  and  $q_t$  are the adsorption capacities of the adsorbent at equilibrium and at time  $t$  (mg/g), respectively.  $k_1$  is the adsorption rate constant according to the pseudo-first-order model (L/min).

The pseudo-second-order was first presented by Ho and McKay [25]. The non-linear form of this model is expressed in equation 6:

$$q_t = \frac{q_e^2 k_2 t}{1 + q_e k_2 t} \quad (6)$$

$$\frac{dq}{dt} = k_2 (q_e - q)^2 \quad (7)$$

The linear form of the pseudo-second-order model can be obtained by integrating equation 7 under the same condition as equation 4 resulting the following equation.

$$\frac{t}{q_t} = \frac{1}{k_2 q_e^2} + \frac{1}{q_e} t \quad (8)$$

The adsorption kinetics parameters based on the pseudo-first-order was calculated based on the linear plot of  $\log(q_e - q_t)$  against  $t$  (equation 5). The adsorption kinetics parameters based on the pseudo-second-order model was calculated according to the linear plot of  $t/q_t$  versus  $t$  (equation 8). The adsorption kinetics parameters based on both models were tabulated in Table 1. It was found that the pseudo-first order model is better in predicting the experiment data rather than the pseudo-second-order model. The correlation coefficient for pseudo-first-order model was bigger than 0.9 both for activated kaolin and TiO<sub>2</sub>/Kaolin composite. This finding suggested that the rate-limiting step for adsorption process was dominated by the physisorption mechanism [28].

Table 1. Adsorption kinetics parameters of procion red.

Adsorbent	Pseudo-first-order			Pseudo-second-order		
	$q_e$ (mg/g)	$k_1$ (min <sup>-1</sup> )	R <sup>2</sup>	$q_e$ (mg/g)	$k_2$ (mg/g min)	R <sup>2</sup>
A-Kao	25.2	0.048	0.911	-137	$7.31 \times 10^{-6}$	0.024
TiO <sub>2</sub> /Kaolin	29.2	0.054	0.943	51.0	$8.63 \times 10^{-5}$	0.317

#### Adsorption isotherm

Study on the modeling of the equilibrium curve with the most appropriate correlation is a crucial aspect in order to optimize the design of the adsorption experiment. Langmuir and Freundlich adsorption isotherm models are the most widely used model to represent the removal of the dye from aqueous medium [27; 29]. Langmuir [30] adsorption isotherm model was developed based on the assumption that the adsorbate can only be adsorbed on the monolayer of the adsorbent surface. The maximum adsorption capacity of the adsorbent reached when all the surface of the adsorbent was occupied by the ion/molecule adsorbate. This model also assumes that between the adsorbate and adsorbent has no interaction with each other. The theoretical equation of the Langmuir isotherm model is presented in equation 9.

$$q_e = \frac{K_L C_e}{1 + K_L C_e} q_{max} \quad (9)$$

where  $q_e$  is the adsorption capacity (mg/g) and  $C_e$  is the equilibrium of procion red concentration (mg/L).  $K_L$ (L/g) and  $q_{max}$ (mg/g) are the constant of Langmuir isotherm correspond to the adsorption energy and monolayer coverage, respectively. In order to evaluate the value of  $K_L$  and  $q_{max}$ , equation 9 can be transformed into its linear form as presented in equation 10 as follow.

$$\frac{C_e}{q_e} = \frac{1}{q_{max} K_L} + \frac{1}{q_{max}} C_e \quad (10)$$

On the other hand, the Freundlich isotherm model considering that the adsorption process probably occurred in the heterogeneous system which is not limited by the formation of the monolayer. This model is mathematically described by the following equation.

$$q_e = K_F C_e^{1/n} \quad (11)$$

where  $K_F$  is the Freundlich constant based on the adsorption capacity (L/mg),  $n$  is the Freundlich constant related to the adsorption intensity.  $1/n$  value can be used to describe the adsorption favorability. When  $1/n$  is equal to zero indicating that the type of adsorption isotherm is irreversible. When  $1/n$  less than 1 and bigger than zero ( $0 < 1/n < 1$ ), the type of the adsorption isotherm is favorable and if the  $1/n$  value is bigger than one ( $1 < 1/n$ ) indicate that the type of adsorption isotherm is unfavourable [31]. Both the Freundlich isotherm constant can be measured from the slope and intercept value of the plot of  $\ln q_e$  versus  $\ln C_e$  from its linear form as follow [32]:

$$\ln q_e = \ln K_F + \frac{1}{n} \ln C_e \quad (12)$$

The adsorption isotherm parameters according to the Langmuir and Freundlich model are summarized in Table 2. Based on the coefficient regression values  $R^2$ , both the Langmuir and Freundlich are in a good agreement to correlate the adsorption equilibrium data. Based on the Freundlich model, the  $1/n$  values for all the temperature studied showed in the range of 0 to 1. This finding described that the adsorption of procion red on TiO<sub>2</sub>/Kaolin composite was in favorable process. Moreover, the  $q_m$  values according to the Langmuir model ranging from 125 to 158 mg/g.

Table 2. Isotherm parameters for procion red adsorption on TiO<sub>2</sub>/Kaolin composite.

Models	Parameters	Temperature (°C)				
		30	40	50	60	70
Langmuir	$K_L$	0.0161	0.0304	0.0571	0.0616	0.0724
	$q_m$	158	137	125	137	153
	$R^2$	0.9711	0.8834	0.9822	0.9532	0.9685
Freundlich	$K_F$	0.171	0.118	11.3	12.7	15.5
	$1/n$	1.32	1.32	0.573	0.5818	0.584
	$R^2$	0.9837	0.9042	0.9365	0.886	0.908

#### Adsorption thermodynamic

In this work, the thermodynamic behavior of procion red adsorption was studied by conducting the adsorption experiment with different temperatures. Effect of temperature on the adsorption performance was evaluated at four different temperatures, i.e., 30, 40, 50, 60, and 70 °C. The results are presented in Figure 6. The obtained data described that by increasing the adsorption temperature, the adsorption capacity gradually increased. This phenomenon also reported by

Kaveeshwar *et al.* [33], as caused by the increase of diffusion rate and adsorbate mobility in the higher temperature.

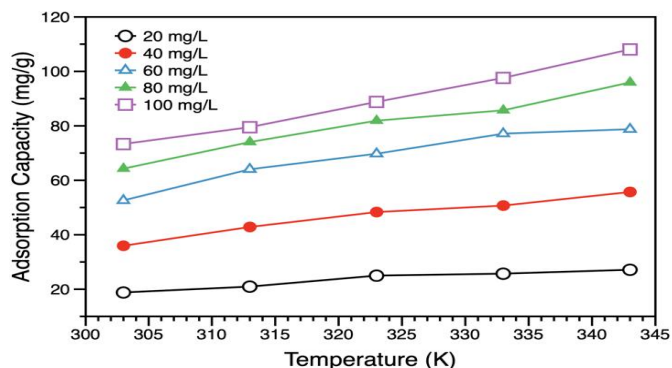


Figure 6. Effect of temperature on the adsorption capacity.

Three basic thermodynamic parameters, including the change of standard enthalpy ( $\Delta H^\circ$ ), change of standard entropy ( $\Delta S^\circ$ ) and the change of Gibbs free energy ( $\Delta G^\circ$ ) were systematically evaluated. These parameters are an essential aspect in order to determine the adsorption behavior of spontaneity, the nature of the adsorption exothermic and endothermic, and how much changes occurred on the surface of the adsorbent [34].

The thermodynamic parameters mentioned above can be calculated based on the following equation [35].

$$K_d = \frac{q_e}{c_e} \quad (13)$$

$$\Delta G^\circ = -RT \ln K_d \quad (14)$$

$$\ln K_d = \frac{\Delta S^\circ}{R} - \frac{\Delta H^\circ}{R} \frac{1}{T} \quad (15)$$

$$\Delta G^\circ = \Delta H^\circ - T\Delta S^\circ \quad (16)$$

where  $K_d$  is the equilibrium constant,  $R$  is the gas constant (8.314 J/mol.K), and  $T$  is the absolute temperature (K). The value of the thermodynamic parameters were measured based on the linear form of equation 15. The value of  $\Delta S^\circ$  and  $\Delta H^\circ$  were the intercept and slope of the linear plot of  $\ln K_d$  against  $1/T$ . The results of thermodynamic parameters measurement based on the adsorption data are presented in Table 3.

The change of Gibbs free energy  $\Delta G^\circ$  for all the experimental condition was recorded negative. This finding showed that the adsorption process was spontaneous in all the setup of experimental condition. Moreover, the negative value of  $\Delta G^\circ$  was gradually increased by increasing the temperature. It was described that the adsorption process is more favorable in higher temperature. The value of  $\Delta G^\circ$  was observed in the range of -0.559 to -5.96 kJ/mol. In which this value describes that the interaction between the procion red and the surface of  $\text{TiO}_2/\text{Kaolin}$  composite is only an electrostatic interaction since the magnitude of  $\Delta G^\circ$  value was less than -20 kJ/mol. According to the paper reported by Munagapati *et al.* [1], the magnitude of  $\Delta G^\circ$  value for the chemisorption ranging from -80 to -400 kJ/mol and for physisorption ranging from 0 to -20 kJ/mol.

The calculated value of the change of enthalpy  $\Delta H^\circ$  also gives more description that the adsorption process was obeyed the endothermic nature as it was observed has positive value in

all the range of adsorption temperature used. The magnitude of the  $\Delta H^o$  values also considers that the adsorption process was obeyed the physisorption mechanism. As can be seen in the Table 3, the magnitude of  $\Delta H^o$  value ranging from 18.5 to 30.3 kJ/mol which these values were less than 80 kJ/mol. Generally, the magnitude of  $\Delta H^o$  value for chemisorption ranging from 80 to 200 kJ/mol [1]. The value of the entropy changes  $\Delta S^o$  was recorded positives for all the experimental condition. This finding indicated that the randomness process was increased during the adsorption occurred.

Table 3. Thermodynamic parameter for procion red adsorption on TiO<sub>2</sub>/Kaolin.

Concentration (mg/L)	T (°C)	$\Delta G$ (kJ/mol)	$\Delta H$ (kJ/mol)	$\Delta S$ (J/mol)	R <sup>2</sup>
20	30	-1.96	27.1	96.1	0.9639
	40	-2.92			
	50	-3.88			
	60	-4.84			
	70	-5.80			
40	30	-1.73	30.3	106	0.9868
	40	-2.79			
	50	-3.85			
	60	-4.90			
	70	-5.96			
60	30	-1.73	26.5	93.2	0.9726
	40	-2.66			
	50	-3.60			
	60	-4.53			
	70	-5.46			
80	30	-1.13	20.7	71.9	0.9807
	40	-1.85			
	50	-2.56			
	60	-3.28			
	70	-4.00			
100	30	-0.559	18.5	62.8	0.9836
	40	-1.19			
	50	-1.81			
	60	-2.44			
	70	-3.07			

## CONCLUSION

In this work, TiO<sub>2</sub>-coated kaolin composite was prepared using thermal, and acid activated kaolin and titanium(IV) isopropoxide as the titanium source. The TiO<sub>2</sub>/Kaolin composite was then used as an adsorbent material for procion red removal from aqueous solution. The experimental parameter studied showed that the procion red adsorption was a pH-dependent process. Compared with activated kaolin, TiO<sub>2</sub>/Kaolin composite adsorbent has higher adsorption capability toward the procion red. The adsorption kinetics investigation indicated that the adsorption process obeyed the pseudo-first-order model rather than the pseudo-second-order model. The isotherm indicated that the adsorption isotherm model was best fitted on the both Langmuir and Freundlich model. The thermodynamic study revealed that the adsorption of procion red on TiO<sub>2</sub>/Kaolin composite was spontaneous and followed the endothermic nature.

## ACKNOWLEDGMENTS

TT profoundly thanks to the Ministry of Research, Technology, and Higher and Education (*Kemenristekdikti*) of Republic Indonesia for the fellowship and financially supporting this research through "Program Magister Menuju Doktor Untuk Sarjana Unggul (PMDSU)" scholarship and research grant with contract number 468/UN9.3.1/LT/2017 and 326/SP2H/LT/DRPM/IX/2016. The authors also thanked to the Universitas Sriwijaya for the support through the "Hibah Profesi" grant with contract number 987/UN9.3.1/PP/2017.

## REFERENCES

1. Munagapati, V.S.; Yarramuthi, V.; Kim, Y.; Lee, K.M.; Kim, D.-S. Removal of anionic dyes (Reactive Black 5 and Congo Red) from aqueous solutions using banana peel powder as an adsorbent. *Ecotoxicol. Environ. Saf.* **2018**, *148*, 601–607.
2. Taher, T.; Rohendi, D.; Mohadi, R.; Lesbani, A. Preparation and characterization of Dabco (1,4-diazabicyclo[2.2.2]octane) modified bentonite: Application for Congo red removal. In *IOP Conference Series: Materials Science and Engineering*, IOP Publishing; **2018**; p. 12055.
3. Nandi, B.K.; Patel, S. Effects of operational parameters on the removal of brilliant green dye from aqueous solutions by electrocoagulation. *Arab. J. Chem.* **2017**, *10*, S2961-S2968.
4. Cotillas, S.; Llanos, J.; Cañizares, P.; Clematis, D.; Cerisola, G.; Rodrigo, M.A.; Panizza, M. Removal of procion red MX-5B dye from wastewater by conductive-diamond electrochemical oxidation. *Electrochim. Acta* **2018**, *263*, 1–7.
5. Adebayo, M.A.; Prola, L.D.T.; Lima, E.C.; Puchana-Rosero, M.J.; Cataluña, R.; Saucier, C.; Umpierrez, C.S.; Vagheti, J.C.P.; da Silva, L.G.; Ruggiero, R. Adsorption of procion blue MX-R dye from aqueous solutions by lignin chemically modified with aluminium and manganese. *J. Hazard. Mater.* **2014**, *268*, 43–50.
6. Bentahar, S.; Dbik, A.; Khomri, M. El; Messaoudi, N. El; Lacherai, A. Removal of a cationic dye from aqueous solution by natural clay. *Groundwater Sustain. Dev.* **2018**, *6*, 255–262.
7. Mahmoud, M.S.; Farah, J.Y.; Farrag, T.E. Enhanced removal of Methylene Blue by electrocoagulation using iron electrodes. *Egypt. J. Pet.* **2013**, *22*, 211–216.
8. Khemila, B.; Merzouk, B.; Chouder, A.; Zidelkhir, R.; Leclerc, J.-P.; Lapique, F. Removal of a textile dye using photovoltaic electrocoagulation. *Sustain. Chem. Pharm.* **2018**, *7*, 27–35.
9. Liu, Y.; Fu, J.; Deng, S.; Zhang, X.; Shen, F.; Yang, G.; Peng, H.; Zhang, Y. Degradation of basic and acid dyes in high-voltage pulsed discharge. *J. Taiwan Inst. Chem. Eng.* **2014**, *45*, 2480–2487.
10. Melo, R.P.F.; Neto, E.L.B.; Nunes, S.K.S.; Dantas, T.N.C.; Neto, A.A.D. Removal of Reactive Blue 14 dye using micellar solubilization followed by ionic flocculation of surfactants. *Sep. Purif. Technol.* **2018**, *191*, 161–166.
11. Chen, C.-Y.; Kuo, J.-T.; Yang, H.-A.; Chung, Y.-C. A coupled biological and photocatalysis pretreatment system for the removal of crystal violet from wastewater. *Chemosphere* **2013**, *92*, 695–701.
12. Wu, J.; Gao, H.; Yao, S.; Chen, L.; Gao, Y.; Zhang, H. Degradation of Crystal Violet by catalytic ozonation using Fe/activated carbon catalyst. *Sep. Purif. Technol.* **2015**, *147*, 179–185.
13. Jana, S.; Purkait, M.K.; Mohanty, K. Removal of crystal violet by advanced oxidation and microfiltration. *Appl. Clay Sci.* **2010**, *50*, 337–341.

14. Mouni, L.; Belkhiri, L.; Bollinger, J.-C.; Bouzaza, A.; Assadi, A.; Tirri, A.; Dahmoune, F.; Madani, K.; Remini, H. Removal of Methylene Blue from aqueous solutions by adsorption on Kaolin: Kinetic and equilibrium studies. *Appl. Clay Sci.* **2018**, *153*, 38–45.
15. Ekosse, G.-I.E.; Mwitondi, K.S. Principal component analysis to evaluate the spatial variation of major elements in kaolin deposit. *Bull. Chem. Soc. Ethiop.* **2015**, *29*, 41–51.
16. Khairy, M.; Ayoub, H.A.; Rashwan, F.A.; Abdel-Hafez, H.F. Chemical modification of commercial kaolin for mitigation of organic pollutants in environment via adsorption and generation of inorganic pesticides. *Appl. Clay Sci.* **2018**, *153*, 124–133.
17. Gao, Z.; Li, X.; Wu, H.; Zhao, S.; Deligeer, W.; Asuha, S. Magnetic modification of acid-activated kaolin: Synthesis, characterization, and adsorptive properties. *Microporous Mesoporous Mater.* **2015**, *202*, 1–7.
18. Ondruška, J.; Csáki, Š.; Trnovcová, V.; Štubňová, I.; Lukáč, F.; Pokorný, J.; Vozár, L.; Dobrošný, P. Influence of mechanical activation on {DC} conductivity of kaolin. *Appl. Clay Sci.* **2018**, *154*, 36–42.
19. Balczár, I.; Korim, T.; Kovács, A.; Makó, É. Mechanochemical and thermal activation of kaolin for manufacturing geopolymer mortars {textendash} comparative study. *Ceram. Int.* **2016**, *42*, 15367–15375.
20. Gao, W.; Zhao, S.; Wu, H.; Deligeer, W.; Asuha, S. Direct acid activation of kaolinite and its effects on the adsorption of methylene blue. *Appl. Clay Sci.* **2016**, *126*, 98–106.
21. Magdy, A.; Fouad, Y.O.; Abdel-Aziz, M.H.; Konsowa, A.H. Synthesis and characterization of Fe<sub>3</sub>O<sub>4</sub>/kaolin magnetic nanocomposite and its application in wastewater treatment. *J. Ind. Eng. Chem.* **2017**, *56*, 299–311.
22. Zhao, X.; Li, J.; Liu, Y.; Zhang, Y.; Qu, J.; Qi, T. Preparation and mechanism of {TiO<sub>2</sub>}<sub>2</sub>-coated illite composite pigments. *Dye. Pigment.* **2014**, *108*, 84–92.
23. Belhouchat, N.; Zaghouane-Boudiaf, H.; Viseras, C. Removal of anionic and cationic dyes from aqueous solution with activated organo-bentonite/sodium alginate encapsulated beads. *Appl. Clay Sci.* **2017**, *135*, 9–15.
24. Lagergren, S. Zur theorie der sogenannten Adsorption gelöster stoffe, Kungliga Svenska Vetenskapsakademiens. *Handlingar.* **1989**, *24*, 1–39.
25. Ho, Y.S.; McKay, G. Pseudo-second order model for sorption processes. *Process Biochem.* **1999**, *34*, 451–465.
26. Okoro, H.K.; Tella, A.C.; Ajibola, O.A.; Zvinowanda, C.; Ngila, J.C. Adsorptive removal of naphthalene and anthracene from aqueous solution with zinc and copper-terephthalate metal-organic frameworks. *Bull. Chem. Soc. Ethiop.* **2019**, *33*, 229–241.
27. Bulut, E.; Özacar, M.; Şengil, I.A. Adsorption of malachite green onto bentonite: Equilibrium and kinetic studies and process design. *Microporous Mesoporous Mater.* **2008**, *115*, 234–246.
28. Hao, Y.F.; Yan, L.G.; Yu, H.Q.; Yang, K.; Yu, S.J.; Shan, R.R.; Du, B. Comparative study on adsorption of basic and acid dyes by hydroxy-aluminum pillared bentonite. *J. Mol. Liq.* **2014**, *199*, 202–207.
29. Malik, P.K. Dye removal from wastewater using activated carbon developed from sawdust: Adsorption equilibrium and kinetics. *J. Hazard. Mater.* **2004**, *113*, 81–88.
30. Langmuir, I. The constitution and fundamental properties of solids and liquids. Part I. Solids. *J. Am. Chem. Soc.* **1916**, *38*, 2221–2295.
31. Mahmoodi, N.M.; Hayati, B.; Arami, M.; Lan, C. Adsorption of textile dyes on Pine Cone from colored wastewater: Kinetic, equilibrium and thermodynamic studies. *Desalination* **2011**, *268*, 117–125.
32. Salem, M.A.; Elsharkawy, R.G.; Hablas, M.F. Adsorption of brilliant green dye by polyaniline/silver nanocomposite: Kinetic, equilibrium, and thermodynamic studies. *Eur. Polym. J.* **2016**, *75*, 577–590.

33. Kaveeshwar, A.R.; Ponnusamy, S.K.; Revellame, E.D.; Gang, D.D.; Zappi, M.E.; Subramaniam, R. Pecan shell based activated carbon for removal of iron(II) from fracking wastewater: Adsorption kinetics, isotherm and thermodynamic studies. *Process Saf. Environ. Prot.* **2018**, *114*, 107–122.
34. Javed, S.H.; Zahir, A.; Khan, A.; Afzal, S.; Mansha, M. Adsorption of Mordant Red 73 dye on acid activated bentonite: Kinetics and thermodynamic study. *J. Mol. Liq.* **2018**, *254*, 398–405.
35. Khosravi, R.; Moussavi, G.; Ghaneian, M.T.; Ehrampoush, M.H.; Barikbin, B.; Ebrahimi, A.A.; Sharifzadeh, G. Chromium adsorption from aqueous solution using novel green nanocomposite: Adsorbent characterization, isotherm, kinetic and thermodynamic investigation. *J. Mol. Liq.* **2018**, *256*, 163–174.